Ab initio investigation of barium-scandium-oxygen coatings on tungsten for electron emitting cathodes

Vasilios Vlahos,[1,*] John H. Booske,[1,2] and Dane Morgan[1,3]
[1]*Interdisciplinary Materials Science Program, University of Wisconsin–Madison, 1509 University Avenue, Madison, Wisconsin 53706, USA*
[2]*Department of Electrical and Computer Engineering, University of Wisconsin–Madison, 1415 Engineering Drive, Madison, Wisconsin 53706, USA*
[3]*Department of Materials Science and Engineering, University of Wisconsin–Madison, 1509 University Avenue, Madison, Wisconsin 53706, USA*
(Received 4 September 2009; published 22 February 2010)

Microwave, x-ray, and radio-frequency radiation sources require a cathode emitting electrons into vacuum. Thermionic B-type dispenser cathodes consist of Ba_xO_z coatings on tungsten (W), where the surface coatings lower the W work function and enhance electron emission. The new and promising class of scandate cathodes modifies the B-type surface through inclusion of Sc, and their superior emissive properties are also believed to stem from the formation of a low work function surface alloy. In order to better understand these cathode systems, density-functional theory (DFT)-based *ab initio* modeling is used to explore the stability and work function of $Ba_xSc_yO_z$ on W(001) monolayer-type surface structures. It is demonstrated how surface depolarization effects can be calculated easily using *ab initio* calculations and fitted to an analytic depolarization equation. This approach enables the rapid extraction of the complete depolarization curve (work function versus coverage relation) from relatively few DFT calculations, useful for understanding and characterizing the emitting properties of novel cathode materials. It is generally believed that the B-type cathode has some concentration of Ba-O dimers on the W surface, although their structure is not known. Calculations suggest that tilted Ba-O dimers are the stable dimer surface configuration and can explain the observed work function reduction corresponding to various dimer coverages. Tilted Ba-O dimers represent a new surface coating structure not previously proposed for the activated B-type cathode. The thermodynamically stable phase of Ba and O on the W surface was identified to be the $Ba_{0.25}O$ configuration, possessing a significantly lower Φ value than any of the Ba-O dimer configurations investigated. The identification of a more stable $Ba_{0.25}O$ phase implies that if Ba-O dimers cover the surface of emitting B-type cathodes, then a nonequilibrium steady state must dominate the emitting surface. The identification of a stable and low work function $Ba_{0.25}Sc_{0.25}O$ structure suggests that addition of Sc to the B-type cathode surface could form this alloy structure under operating conditions, leading to improved cathode performance and stability. Detailed comparison to previous experimental results of $Ba_xSc_yO_z$ on W surface coatings are made to both validate the modeling and aid in interpretation of experimental data. The studies presented here demonstrate that *ab initio* methods are powerful for understanding the fundamental physics of electron emitting materials systems and can potentially aid in the development of improved cathodes.

DOI: 10.1103/PhysRevB.81.054207 PACS number(s): 71.15.Mb, 79.40.+z, 73.30.+y, 73.20.At

I. INTRODUCTION

Electron emission cathodes are key components in vacuum electron devices and high-power microwave sources utilized in both civilian and military applications (e.g., satellite and cellular communications, radar, industrial heating and domestic microwave ovens, electronic countermeasures, and directed beam-energy weapons).[1] Cathodes generate the electron beam whose propagation and velocity modulation in an evacuated electromagnetic traveling or standing-wave structure produces microwave energy. In addition, vacuum cathodes are essential in vacuum devices that do not produce electromagnetic radiation, such as field-emission displays, electron microscopes, and electron-beam lithography systems.[2]

Electron emission is a function of the chemical condition of the material surface and is strongly affected by the surface work function, Φ. Φ is defined by

$$\Phi = E_{VAC} - E_F, \tag{1}$$

where E_F is the Fermi level (electron chemical potential) of the material and E_{VAC} the electron vacuum energy level. E_{VAC} is the energy of an electron at rest far enough away from the surface so that electrostatic image-charge restoring forces exerted on the electron by the surface are negligible. Low-Φ materials emit electrons into vacuum more easily than higher-Φ materials and are therefore highly desirable for use as vacuum cathodes.

An important mechanism by which the electron emissive performance of a material system may be enhanced is the formation of a surface-dipole layer due to the presence of a thin, strongly ionic surface coating.[3] The interactions between the dipole coating layer(s) with the substrate modify the surface-potential barrier for electron emission, changing Φ. Dipole-induced Φ lowering is the physical mechanism by which a low-Φ surface is produced in thermionic B-type dispenser cathodes,[4,5] the most common cathode in modern

commercial microwave vacuum electronic devices. More specifically, a Φ reducing barium-oxygen (Ba-O) dipole monolayer is formed on the surface of the porous tungsten (W) substrate, whose pores are filed with a barium-containing emissive compound that, upon operation, supplies Ba to the cathode surface. Thin ionic film coatings yielding strong surface dipoles[6] may also be responsible for the improved emission characteristics of novel field-emission materials such as alkali-halide-coated carbon (C) fiber cathodes.[7]

To optimize existing and develop new surface coatings for electron emission cathodes, it is important to better understand and predict the role of the surface-coating layers on the emissive properties of the cathode. In particular, two of the most essential properties to be predicted are a coating's impact on Φ and its overall stability under cathode operating conditions. *Ab initio* methods can be powerful predictive tools for the determination of both Φ and stability. We will show that *ab initio* results can capture both the effect of surface dipoles on Φ and the so-called depolarization effects associated with having interacting dipoles on a surface. We will demonstrate how a simplified analytic model can be used, in conjunction with calculations, to efficiently and accurately predict depolarization effects, net dipole moments (μ), and effective polarizabilities (α) associated with isolated surface atoms or molecules. We will also describe an approach to obtain the stability of complex surface-coating layers appropriate to cathode applications. We will then use the surface-energy stability model to demonstrate that the thermionic dispenser B-type (Ba-O monolayers on W) cathode likely operates in a nonequilibrium steady state quite different from that expected under thermodynamically equilibrium conditions. Finally, we will give a detailed comparison between theory and experiments, focusing on the Φ value of $Ba_xSc_yO_z$ alloy surface coatings on W (where x, y, and z are the number of Ba, Sc, and O atoms, respectively, per surface W atom), demonstrating the power of the calculation approach to aid in the interpretation of experimental data.

This work will focus on systems consisting of $Ba_xSc_yO_z$ alloy surface coatings on a W(001) substrate. There are three motivations for studying this system. First, the properties of this system can be usefully compared and contrasted with those of the Ba_xO_z on W system, characteristic of thermionic B-type dispenser cathodes. B-type cathodes and Ba_xO_z films on W have been extensively investigated during the past 30 years and consequently this electron emission material and its thin-film structures are well characterized and understood systems. Second, scandate cathodes, consisting of $Ba_xSc_yO_z$ alloy surface coatings on W are a new and very promising thermionic electron emission technology. Finally, experimental studies of Φ versus alloy surface coverage for different suballoys of $Ba_xSc_yO_z$ on W(001) are available for careful comparison to our calculations.

Section II describes the computational methods applied, the theory of depolarization, and the method for calculating the surface stability of alloy structures. In addition, Sec. II also reviews and summarizes the current understanding about the surface structure and composition of thermionic dispenser B-type cathodes. Section III A describes calculation of depolarization effects and how combining *ab initio* and analytic models can be an effective tool for capturing these effects. Section III B describes studies of stability for $Ba_xSc_yO_z$ coatings, including implications for steady-state stabilization of nonequilibrium B-type cathode surfaces, and discusses how alloying may impact Φ. Section III C provides a detailed comparison of results obtained by modeling with those obtained experimentally. Finally, Sec. IV summarizes the key findings and provides conclusions.

II. COMPUTATIONAL METHODS AND THEORETICAL BACKGROUND

A. *Ab initio* methods

This work utilizes *ab initio* quantum-mechanical modeling, as implemented in the Vienna *ab initio* simulation package (VASP),[8] to obtain a fundamental understanding of the electronic properties and structural stability of cathode surfaces with $Ba_xSc_yO_z$ monolayer-type alloy surface coatings on the W(001) substrate. The simulations were performed using density-functional theory (DFT) (Ref. 9) in the generalized gradient approximation (GGA),[10] with a plane-wave basis set utilizing the projector-augmented wave (PAW) (Ref. 11) method. We used potentials with electronic configurations of Ba ($5s^2$ $5p^6$ $6s^2$), Sc ($3p^6$ $4s^2$ $3d^1$), O ($2s^2$ $2p^4$), and W ($5p^6$ $6s^2$ $5d^4$). The $Ba_xSc_yO_z$ alloy systems investigated were arranged in periodic supercell slab geometries consisting of five atomic layers of W substrate plus coating layers on the terminating surface. Beyond the surface of the material, a 20–25 Å vacuum region normal to the surface plane was utilized. The electron vacuum energy, E_{VAC}, was well converged with respect to vacuum thickness. The bottom two W layers of the substrate served as the bulk and were frozen into bulk positions while the topmost three W layers and any $Ba_xSc_yO_z$ coating layers were allowed to fully relax to the nearest local minimum or saddle point. K-point sampling in the Brillouin zone was performed using $16\times16\times2$ Monkhorst-Pack[12] mesh grids for unit cells of dimensions 3.19 Å $\times$ 3.19 Å $\times$ 32 Å (this is the dimension of the 1×1 conventional bcc W unit cell along the (100) and (010) directions in the slab geometry with vacuum normal to the terminating surface). The k-point density in reciprocal space was kept as constant as possible when varying the size of the supercell. A cutoff energy of 325 eV was used for all $Ba_xSc_yO_z$ on W(001) calculations. Surface structure formation energies and Φ values were converged to within approximately 30 and 100 meV per surface W atom correspondingly, with respect to the number of W atomic layers, vacuum thickness, k points, and energy cutoff. All calculations reported were performed without spin polarization. Select structures were explored with spin-polarized calculations and no magnetic moment was found to be stable.

In order to establish the accuracy of the calculations, we compared the computational Φ values with those reported from experiments for a selective list of pure metals. The experimental Φ values of the metals investigated have been well documented and the metals possess simple crystal structures, making direct comparison between the calculations and experiment straightforward. The same k points, slab geometries, and relaxation scheme as for the alloy surface

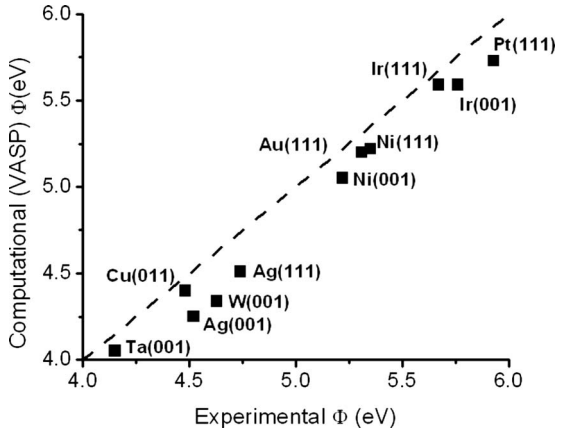

FIG. 1. Comparison between *ab initio* calculated and experimentally measured (from Ref. 14) work function, Φ, values for a selective list of single-element metallic materials relevant to cathode applications. The comparison serves to establish error bars for our calculations of Φ. The theoretical data points were obtained using the PAW GGA implementation.

structures on W were also utilized during this investigation. However, systems with hexagonal unit-cell geometry utilized gamma-centered mesh grids.[13] During this investigation, the cutoff energy was set to a value 30% higher than the maximum cutoff energy associated with the pseudopotentials utilized. Figure 1 compares the Φ values obtained computationally from fully relaxed single-element metallic systems to experimental values.[14] The largest difference in Φ between theory and experiment is less than 0.3 eV and the overall root-mean-square (rms) deviation is 0.2 eV. Given the ability to predict well the Φ values in simple metal systems, we now provide a detailed comparison of predicted and measured Φ values for the $Ba_xSc_yO_z$ surface-coating layer structures.

B. Surface dipoles and the depolarization model

Understanding and calculating the impact of a surface layer on Φ is made more complex by the phenomenon of depolarization. Consider, for example, a W surface covered by Ba-O dipoles. The simplest approach for predicting the dipole moment at a specific surface coverage would be to determine the dipole moment of a single Ba-O dipole and then use that value to predict the dipole moment at any coverage. However, dipoles on the surface interact with each other electrostatically to reduce the dipole moment of each Ba-O molecule, especially at a high surface coverage. This reduction in dipole moments for a given surface atom or molecule, due to electrostatic interactions with other surface atoms or molecules, is called depolarization. Since depolarization depends on coverage and, potentially, on the exact configuration of the surface dipoles, it might seem that one must calculate the dipole moment for every coverage and configuration of interest. However, by combining relatively simple analytical models with a few well-chosen calculations, it is possible to predict with good accuracy the local dipole strengths, depolarization, and the overall Φ changes for any given surface-dipole coverage. To explain the approach used in this work and to introduce relevant terminology we provide a brief review below.

Thin-film coatings of alkali metals or oxides can significantly modify the Φ of the bare substrate. Langmuir[15] was the first to conduct systematic studies of this effect by investigating the change in Φ of a W surface upon exposure to vapors of metallic cesium (Cs). He attributed the reduction in Φ to the ionization of the Cs adatoms, proposing that the ionized adatoms, in conjunction with their image charge in the metal, induce a surface dipole that lowers the electrostatic potential barrier of the surface. The change in work function, $\Delta\Phi$, ($\Delta\Phi = \Phi_{\mathrm{FINAL}} - \Phi_{\mathrm{INITIAL}}$) as a function of the dipole surface density is described by the Helmholtz equation,[3,16]

$$\Delta\Phi = \frac{-e}{\varepsilon_0}\mu_z(N)N, \tag{2}$$

where N is the number of surface-coating molecules per unit area, $\mu_z(N)$ is the dipole moment per molecule along the z direction (normal to the emitting surface), and ε_0 is the permittivity of free space. $\mu_z(N)$ is the normal component of the true dipole moment of the real charges of the system without contributions from image charges. Inclusion of image charges would necessitate a correction of Eq. (2) by a factor of 2, as is done in some texts.[3] It can be seen that the relation between the reduction in the work function, $\Delta\Phi$, and the net normal dipole moment per unit area (dipole surface density), $\mu_z(N)N$, is linear with a slope of -181 eV Å$/e$.

Depolarization occurs because the electric field from surrounding dipoles modifies the local dipole according to

$$\mu_z = \mu_{0z} + \alpha E_z, \tag{3}$$

where E_z is the z component of the electric field generated by all other dipoles in the system (note that E_z is a negative quantity when the field direction is opposite that of the dipole moment μ_{0z}). μ_{0z} is the surface-normal dipole moment in the limit of very low surface coverage, where no depolarization is present and α is the polarizability of the surface dipoles. The z component of the electric field induced by another surface dipole of magnitude μ_z at a distance R is given by

$$E_{DEP(z)} = \frac{-\mu_z}{4\pi\varepsilon_o}\frac{1}{R^3}. \tag{4}$$

We expect the interdipole separation R to scale approximately as $R \propto 1/N^{1/2}$, which means $E_{DEP(Z)} \propto \mu_z N^{3/2}$. Equation (4) can then be rewritten as

$$E_{DEP(z)} = c\frac{-\mu_z N^{3/2}}{4\pi\varepsilon_o}, \tag{5}$$

where c is an unknown parameter for any given surface coverage. Solving Eqs. (3) and (5) for μ_z, and then substituting the result into Eq. (2), yields the expression

$$\Delta\Phi = \frac{-1}{\varepsilon_O}\frac{eN\mu_{0_z}}{1+(caN^{3/2})/(4\pi\varepsilon_0)}. \quad (6)$$

In general, c in Eq. (6) will depend on the exact configuration of the dipoles. For a square and triangular network of dipoles, the exact values of c are 9.0336 and 8.8927, respectively.[3,17] The fact that these values are so close suggests that $c=9$ might be a generally good approximation for the c value. This estimate for c is useful for finding the polarizability, α, from fits which yield $c\alpha$ (see Sec. III A).

Equation (6) is the "classic" depolarization equation, describing the reduction in Φ for a system having a precisely known surface-coating coverage. Note that there are a number of assumptions in this derivation, including that there is only one type of dipole, that the dipole responds linearly to local fields, and that there are no changes in the dipole moments with coverage except their linear response to each other's electrostatic fields (e.g., it is assumed that dipoles do not turn over during changes in coverage or start interacting through direct bonding). These assumptions must be met for Eq. (6) to hold. If the terms $c\alpha$ and μ_{0z} are known in Eq. (6), then the depolarization properties of the system can be predicted. If $c\alpha$ and μ_{0z} are not known, then they can be fit to match experimental or calculated values for Φ versus coverage. Once a fit has been performed, Eq. (6) can be used to predict Φ quickly for any coverage. *Ab initio* simulations in combination with the depolarization model of Eq. (6) can be utilized to rapidly generate the entire depolarization curve of Φ as a function of coverage. It will be shown in Sec. III A that only a few calculated points are needed to effectively generate the entire depolarization curve. By fitting to Eq. (6), it is also possible to extract the values of $c\alpha$ and μ_{0z}, which help to characterize the fundamental properties of the surface-dipole layer. Combining *ab initio* calculations and Eq. (6) can be much more efficient than direct calculation of many dipole surface coverages.

C. Stability

Calculating the formation energy, ΔE_F, is a powerful tool for determining the structure and composition of plausible multicomponent alloy surface coatings. For cathodes we must work with an "open" system, where we define an open system as one that can exchange atoms with an external reservoir (a grand canonical ensemble). The determination of the formation energy in open systems enables the direct comparison of the thermodynamic stability of complex structures having different stoichiometry.

In this paper, we wish to determine the stability of $Ba_xSc_yO_z$ surface-alloy structures consisting of a monolayer (or a few layers) on a W(001) substrate. The formation energy of $Ba_xSc_yO_z$ surface structures from their respective Ba, Sc, and O sources is computed using Eq. (7),

$$\Delta E_F[Ba_xSc_yO_z|W(001)] = E[Ba_xSc_yO_z|W(001)] - E[W(001)] - x\mu_{Ba} - y\mu_{Sc} - z\mu_O. \quad (7)$$

In Eq. (7), E is the total energy of a specific fully relaxed alloy structure, x, y, and z are the number of Ba, Sc, and O atoms per W surface atom, respectively, and μ_i is the chemical potential per atom of the source reservoir corresponding to the species I (where I can be either Ba or Sc or O). Because we are interested in the formation energy of different $Ba_xSc_yO_z$ surface complexes decorating the same underlying W(001) substrate, Eq. (7) removes the contributions of the latter by subtracting the calculated total energy of the W substrate from the total energy of the system [this is the E[W(001)] term]. The chemical potential of O can be obtained from experimental thermodynamic data for oxygen gas under cathode operating conditions. However, the chemical potentials for Ba and Sc are not known under the cathode operating conditions. In order to estimate the chemical-potential terms in the expression, it is assumed that Ba and Sc are drawn from their stable binary oxides, BaO and Sc_2O_3, respectively. The argument for these reservoirs is that, regardless of how Ba and Sc are introduced to the surface, a reservoir of these elements near equilibrium will form oxides that must be broken up to form the surface layer. Ba and Sc metal are not stable at the relevant P_{O_2} in this study (down to partial pressures of 10^{-8} Torr). Note that no ternary $Ba_xSc_yO_z$ reference compounds were considered in this investigation, as study of the effects of these more complex ternary-alloy reservoirs on surface stability is beyond the scope of this work. Under operating conditions it is possible that kinetic limitations, or more complex alloying, may mean that Ba and Sc are drawn from a source with chemical potentials that differ from those of simple oxide. These differences would shift our formation energies, possibly suggesting different stable stoichiometries. However, we believe the simple oxide reservoirs will give qualitative guidance for the stabilities of different surface structures near equilibrium, and that major discrepancies with experiment can be taken to imply significant deviations from equilibrium behavior. The chemical potentials for Ba, Sc, and O can be derived approximately from the following thermodynamic expressions:

$$\mu_{Ba} = \frac{\partial E}{\partial N_{Ba}} = E(BaO) - \mu_O, \quad (8)$$

$$\mu_{Sc} = \frac{\partial E}{\partial N_{Sc}} = \frac{1}{2}[E(Sc_2O_3) - 3\mu_O], \quad (9)$$

$$\mu_O(T,P) = \frac{1}{2}\left\{E(O_2) + \delta h^0 O_2 + [H(T,P^0) - H(T^0,P^0)] - TS(T,P^0) + kT\ln\left(\frac{P}{P^0}\right) - [G_{s,vib}(O_2,T) - H_{s,vib}(O_2,T_0)]\right\}. \quad (10)$$

Here N_I is the number of atoms corresponding to the specie I, T the operating temperature, T^0 the temperature at standard conditions (T^0=298 K), P the oxygen partial pressure, P^0 the oxygen partial pressure at standard conditions (P^0=0.2 atm), H the gas enthalpy for the given T and P conditions, S the gas entropy for the given T and P condi-

tions, and k is Boltzmann's constant. The $E(\mathrm{BaO})$ and $E(\mathrm{Sc_2O_3})$ terms included in the chemical-potential expressions for Ba and Sc [Eqs. (8) and (9), respectively] correspond to the total bulk energies of the solid BaO and $\mathrm{Sc_2O_3}$ structures which are obtained from fully relaxed bulk calculations. μ_0 is the chemical potential for the oxygen referenced to the pseudoatom that is used in the calculations. The expression for μ_0 in Eq. (10) is the experimental value for oxygen but shifted to account for solid phase vibrations as well as to take into account errors associated with the *ab initio* treatment of the oxygen.[18–20] Definitions of the terms in Eq. (10) can be found in Ref. 20. Note that the O contribution to the solid-phase vibrational free energy is approximated with a simple Einstein model with the Einstein frequency θ_E=500 K. 500 K is an approximate value but changing it by a factor of 2 in either direction (from 250 to 750 K) does not qualitatively impact any of our conclusions so no effort is expended on a more rigorous quantitative model.

Substituting Eqs. (8)–(10) into Eq. (7) yields an expression for the formation energy of a $\mathrm{Ba}_x\mathrm{Sc}_y\mathrm{O}_z$ surface layer in terms of known or easily calculated quantities,

$$\Delta E_F[\mathrm{Ba}_x\mathrm{Sc}_y\mathrm{O}_z|\mathrm{W}(001)] = E[\mathrm{Ba}_x\mathrm{Sc}_y\mathrm{O}_z|\mathrm{W}(001)] - E[\mathrm{W}(001) - xE(\mathrm{BaO})] - \frac{1}{2}yE(\mathrm{Sc_2O_3}) + \left(x + \frac{3}{2}y - z\right)\mu_{\mathrm{O}}. \quad (11)$$

The chemical potentials of Ba and Sc have now been conveniently replaced by the total energies of their source reference states, namely, BaO and $\mathrm{Sc_2O_3}$, which can be extracted directly from the calculations. The ΔE_F per $\mathrm{Ba}_x\mathrm{Sc}_y\mathrm{O}_z$ configuration is used to assess the stability of all possible $\mathrm{Ba}_x\mathrm{Sc}_y\mathrm{O}_z$ alloy surface structures. The operating conditions utilized, namely, temperature T=1200 K and pressure $P_{\mathrm{O}_2}=10^{-8}$ Torr, are typical for scandate cathode materials.[21] The subscripts x, y, and z are normalized to be per surface layer W atom so a value of one corresponds to one monolayer (one monolayer=1 ML $=9.85\times10^{14}$ atoms/cm^2).

D. Emitting surface of impregnated dispenser B-type thermionic cathodes

Thermionic B-type dispenser cathodes are of significant technological interest and provide a relatively well-understood cathode system for the comparison to *ab initio* studies. The origin of the Ba-O surface-dipole model, which lowers Φ and explains the operation of thermionic dispenser B-type cathodes, can be traced to the work of Forman[4,22] and Haas *et al.*[5] Forman recorded the auger spectra of an activated B-type cathode at 1100 °C and compared the spectra to those obtained from a $\mathrm{Ba}_x\mathrm{O}_z$ monolayer surface structure grown on a polycrystalline W filament, using the technique of Moore and Allison.[23] Moore and Allison demonstrated that thick Ba films deposited on a W substrate can be converted to Ba-O surface monolayer films by heating the W substrate at 1000 K for 1–3 min. Forman heated the polycrystalline W filament covered with a Ba film for 1 min and noticed that the auger spectra from the polycrystalline filament were the same as those from the activated cathode surface. The effective Φ values measured in both material systems at elevated temperatures (1100 °C for the cathode and 1000 K for the thin-film structure) were also found to be the same. Forman concluded that the surface of the active cathode contained a partial monolayer (~0.5 ML) of Ba and O, most likely as Ba on O on W, in support of a $\mathrm{Ba_{0.5}O_{0.5}}$ monolayer surface model of the hot cathode surface [see Fig. 2(a)]. Haas *et al.* performed a similar investigation by comparing the auger spectra of activated B-type cathodes with those from $\mathrm{Ba}_x\mathrm{O}_z$ thin films grown on a W(001) substrate. They noticed that both spectra were the same at a certain surface coverage of Ba and O on the W film surface, which was identified to be 0.5 MLs of Ba by means of low-energy electron diffraction (LEED). The LEED pattern suggested that the surface Ba is arranged in a structure having an ordered $c(2\times2)$ surface geometry. Although Haas *et al.* recognized that the exact position of the surface Ba atoms with respect to the underlying W(001) substrate cannot be determined by LEED alone, they proposed a possible surface geometric arrangement for the surface dipole with the Ba atoms occupying alternating hollow sites on the surface of W(001) and the O atoms occupying the remaining hollow sites of the surface, yielding a dense fully packed surface film [see Fig. 2(b)]. Consequently, Haas *et al.* concluded that the activated

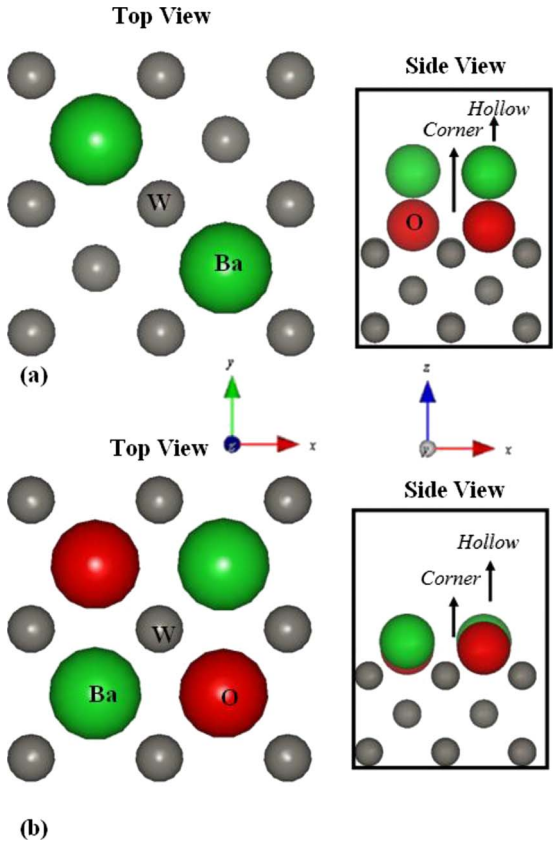

FIG. 2. (Color online) Top and side views of proposed surface geometries for the Ba and O on a W(001) plane: (a) upright (normal) Ba-O dimer over alternating fourfold hollow sites on W and (b) coplanar Ba and O on alternating fourfold hollow surface sites on W. Both structures have stoichiometry $\mathrm{Ba_{0.5}O_{0.5}}$.

surface of a dispenser B-type cathode can be modeled by a $Ba_{0.5}O_{0.5}$ surface monolayer. The reduction in Φ was attributed to the formation of a Ba-O surface-dipole layer.

The local geometry of the Ba_xO_z surface-dipole layer on the surface of the thermionic B-type cathode was investigated by two groups using surface-extended x-ray-absorption fine-structure analysis but they proposed different surface structures based on their experimental results. Norman *et al.*[24] investigated the surfaces of activated dispenser B-type cathodes, both at a nominal operating temperature of 1155 K as well as at room temperature, and concluded that the surface consists of Ba-O dipoles oriented normal with respect to the underlying W substrate, with O on the W surface and Ba above it, and most likely with O occupying the hollow surface sites of the W substrate [see Fig. 2(a)]. The bond-length values and the coordination numbers were averaged over an unknown distribution of crystal faces, due to the polycrystalline nature of the true cathode surface, and a weighted mean value for the Ba neighbor distances had to be utilized in the analysis. The challenges of analyzing polycrystalline data with many surfaces was avoided by Shih *et al.*,[25] who investigated the surface structure of a $Ba_{0.5}O_{0.5}$ monolayer film deposited on W(001) at 860 °C. Their results suggest a different dimer surface geometry than the one proposed by Norman *et al.* [see Fig. 2(b)]. According to the model of Shih *et al.*, the Ba and O atoms lie approximately flat on the plane of the W(001) surface occupying alternating fourfold hollow sites (in a manner analogous to the surface structure proposed by Haas *et al.*[5]). LEED measurements performed on the thin-film structures suggested the presence of an ordered Ba $c(2\times2)$ surface geometry. In Sec. III B, the above-proposed Ba_xO_z surface structures are analyzed in light of their predicted stability and Φ values.

III. RESULTS AND DISCUSSION

A. Modeling depolarization as a function of surface coverage

A series of monomer and normally oriented dimer surface coatings [of the configuration type shown in Fig. 2(a)] have been investigated in order to (i) compare results obtained by modeling to those predicted by the classical depolarization equation [Eq. (6)], (ii) assess how the classical depolarization equation can be used in conjunction with modeling results to effectively reduce the number of required calculations necessary for characterizing dipole-induced Φ changes in a system, and (iii) demonstrate how the calculations and Eq. (6) can be used to determine the effective polarizability α and the noninteracting surface-dipole moment value μ_{0z} of the materials systems under investigation. These calculations will make use of Ba-O dimers on the surface as these have been proposed as a likely structure for the B-type cathode[5,22,24–29] (see Sec. II D). In Sec. III B, we compare Ba-O dimers that are normal to the W surface with tilted dimers and show that the tilted structures are significantly more stable. However, the tilted dimers begin to interact by direct bonding (rather than just electrostatics) at high coverage (see Sec. III B), and therefore do not meet the assumptions made in deriving the depolarization equation [Eq. (6)] for high coverages. Therefore, for the present goal of exploring the depolarization equation and its domain of applicability over a wide range of coverage, only the normal Ba-O dimers over W(001) hollow sites [see Fig. 2(a)] are included.

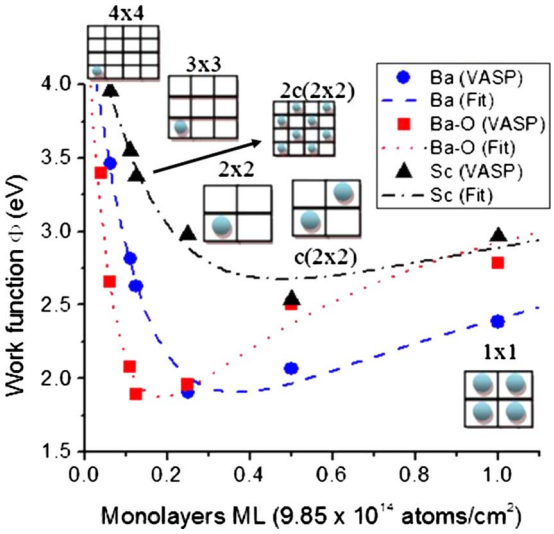

FIG. 3. (Color online) Work function, Φ, versus dimer/monomer surface coverage for Ba and Sc monomers and Ba-O normal dimer configurations on W(001). The data points represent the *ab initio* calculations while the curves are obtained by the depolarization equation [Eq. (6)] utilizing the $c\alpha$ and μ_{0z} values extracted from the optimal fit to all *ab initio* data.

In order to explore how well Eq. (6) can describe *ab initio* data, the approach will be to fit Eq. (6) to the calculated $\Delta\Phi$ versus coverage results obtained by calculations, using $c\alpha$ and μ_{0z} as adjustable parameters to obtain the best possible fit. A good fit will validate the depolarization model and allow the extraction of the $c\alpha$ and μ_{0z} parameters. It will be shown that a similar quality fit to that obtained using many data points can also be obtained through using only a few data points, demonstrating that Eq. (6) is a powerful tool for interpolating between calculations.

The model parameters are determined with a least-squares fit of the calculated change in Φ at coverage N, $\Delta\Phi_{abinit}(N)$, to the change in Φ predicted by Eq. (6), $\Delta\Phi_{depol}(N,\alpha,\mu_{0z})$. The least-squares fit is obtained by minimizing the rms error, defined by

$$\text{rms} = \sqrt{\sum_{i=1}^{n} [\Delta\Phi_{abinit}(N_i) - \Delta\Phi_{depol}(N_i,\alpha,\mu_{0z})]^2/n}. \tag{12}$$

Figure 3 shows the calculated and fit values of $\Delta\Phi$ for the W(001) surface induced by Ba and Sc monomers as well as normal Ba-O dimers, as a function of surface coverage, expressed in monolayers. All arrangements are for a square grid with the monomer or dimer occupying one of the fourfold hollow surface sites. rms error values obtained from the fit are typically less than 0.2 eV and the largest (worst case) errors in the $\Delta\Phi$ fit are never more than 6% different than the *ab initio* $\Delta\Phi$ values for the cases tested. Table I shows the values of $c\alpha$ and μ_{0z} extracted from the fits as well as the value of μ_{0z} obtained from the lowest coverage calculation

TABLE I. Extracted μ_{0z} and $c\alpha$ parameter values (obtained from fitting the theoretical data points to the classical depolarization equation) compared to the theoretical values obtained by *ab initio* modeling. The dipole moment μ_{0z} values are expressed in units of e Å while the polarizability $c\alpha$ is expressed in units of Å^3. The columns refer to three different fits, including one to all the *ab initio* data (6 pt), one to just two high-coverage structures (1×1 and 2×2), and one to just two structures of significantly varying coverage (1×1 and 4×4). See text for more detailed discussion of the fits.

Configuration	μ_z VASP (4×4) (e Å)	μ_{0z} fit (6 pt) (e Å)	$c\alpha$ fit (6 pt) (Å^3)	μ_{0z} fit ($1\times1,2\times2$) (e Å)	$c\alpha$ fit ($1\times1,2\times2$) (Å^3)	μ_{0z} fit ($1\times1,4\times4$) (e Å)	$c\alpha$ fit ($1\times1,4\times4$) (Å^3)
Ba-W	0.756	0.742	9	0.821	10	0.738	9
Ba-O-W	1.448	1.486	25	1.206	18.8	1.414	21.9
Sc-W	0.337	0.407	6	0.437	7.1	0.437	6.9

performed, corresponding to a 4×4 supercell along (001) and (010) (containing 80 W atoms). The ability to extract the isolated μ_{0z} value from fitting Eq. (6) is useful as the noninteracting dipole moment, μ_{0z}, can otherwise only be obtained from large unit-cell calculations which are quite slow with *ab initio* methods. Note that the fit yields only the product $c\alpha$, rather than α directly. However, using the approximate value of $c=9$, the value of α can be estimated (see Sec. II A).

For the Ba configurations investigated, the lowest Φ ($\sim$1.9 eV) is realized for a Ba monomer surface coverage of 0.25 ML, corresponding to one dipole per 2×2 supercell configuration (see inset of Fig. 3 for the schematic of the relevant structure). With the square lattices that were modeled, this yields a nearest-neighbor interdipole separation of 6.37 Å. For the Ba-O configurations investigated, the lowest Φ ($\sim$1.92 eV) is realized for normal Ba-O dimers of 0.125–0.25 ML coverage, corresponding to one dipole per $2c(2\times2)$ or 2×2 supercell configurations, respectively, and yielding a nearest-neighbor interdipole separation of 9.01 Å and 6.37 Å, respectively. Finally, for the Sc configurations, the lowest Φ ($\sim$2.3 eV) is realized for a monomer coverage of 0.5 ML, corresponding to one dipole per $c(2\times2)$ configuration and yielding a nearest-neighbor separation of 4.51 Å. Denser dipole surface-coverage configurations than those cited above yield higher Φ's due to pronounced depolarization[30] (i.e., dipole-dipole repulsion). Diffuse dipole surface coverages also yield higher Φ values due to insufficient coverage of the surface by dipoles resulting in an overall weak dipole moment per unit surface area.

In order to explore the dependence of depolarization on the configuration of a surface, we consider three supercell surface configurations of Ba monomers on W (see Fig. 4). All three configurations illustrated contain a Ba surface coverage of exactly 0.5 MLs but differ in their local Ba arrangements. The Φ values for all three configurations are within 0.1 eV of one another. This result suggests that the dependence of depolarization on a given surface configuration is weak, although other systems or specific configurations may behave somewhat differently.

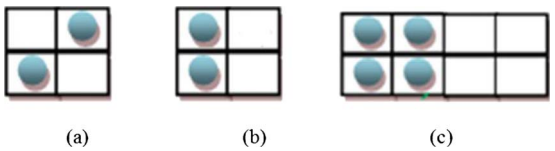

FIG. 4. (Color online) Configurational dependence of depolarization. The three Ba on W(001) structures of exactly 0.5 ML surface coverage have Φ values of (a) 2.08 eV, (b) 2.09 eV, and (c) 2.18 eV. The circles represent Ba atoms placed on the W(001) surface.

The good agreement between *ab initio* and classical depolarization modeling suggest that just a few data points obtained by *ab initio* techniques could be used in conjunction with the classical depolarization theory to accurately generate entire depolarization curves (at least for cases that meet the conditions of applicability of the depolarization theory (see Sec. II B)]. To assess how few data points are needed to fit an accurate depolarization curve, we have performed fits with subsets of the total calculated data. Table I also includes the values of the fitting parameters μ_{0z} and $c\alpha$ obtained from the fitting technique by utilizing only two *ab initio* data points (see last four columns in Table I). In the first test, *ab initio* data points for fitting are obtained from the 1×1 and 2×2 supercell structures, consisting of 5 W and 20 W atoms, respectively. In the second test, *ab initio* data points for fitting are obtained from the 1×1 and 4×4 structure values, consisting of 5 W and 80 W atoms, respectively. It is encouraging to see that qualitatively good agreement with the best μ_{0z} and $c\alpha$ values (obtained from fitting all the *ab initio* data and included in the second and third columns of Table I) can be obtained by fitting just two *ab initio* data points. The overall rms errors for all data points (including those not used in the fit) are less than 0.30 eV for the fit using the 1×1 and 2×2 *ab initio* data points, and less than 0.23 eV for the fit using the 1×1 and 4×4 *ab initio* data points. Fitting the depolarization curve to fewer data points is clearly more efficient since it requires fewer calculations. In addition, the depolarization curve obtained by fitting to the data from high surface-coverage configurations is particularly efficient, as these configurations can be modeled with a smaller cell size and therefore calculated more quickly by *ab initio* methods. Fitting to 1×1 and 2×2 structures is therefore the least computationally demanding approach to obtain the depolarization curve but this fit leads to somewhat higher errors than the fit to the 1×1 and 4×4 structures. In general, fitting data points that include both high and low coverage configurations (small and large size supercells) will likely reproduce the depolarization curve with greater accuracy than using only high-coverage surface configurations but at the expense of more computing time. Overall, the ability to use fewer *ab initio* data points (in this example two

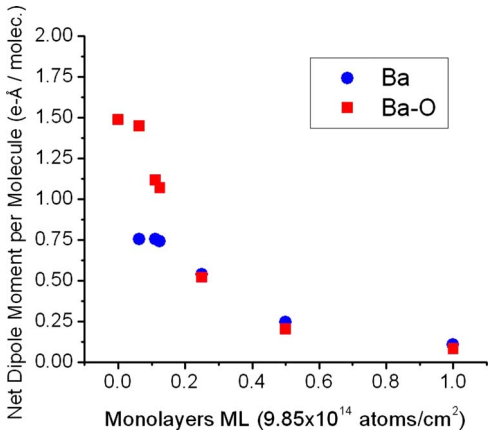

FIG. 5. (Color online) Net dipole moments per molecule (Ba monomer or normal Ba-O dimer) as a function of monomer/dimer surface coverage. Whereas the net dipole moment of the Ba monomer on W has converged at a surface coverage of 0.111 ML, the net dipole moment of the Ba-O dimer has not converged even at a surface coverage of 0.0625 ML.

instead of six total calculated data points) can significantly speed up the generation of complete depolarization curves for a given material system and facilitate the rapid and accurate extraction of important physical parameters (i.e., Φ, α, and μ_{0z}).

As an example of the challenges involved in obtaining μ_{0z} directly, Fig. 5 shows the calculated dipole moments per molecule as a function of surface coverage for Ba monomers and Ba-O dimers on the W(001). The dipole moment for the Ba monomer configurations stops changing significantly below a surface coverage of $\sim$0.111 MLs (3×3 surface size supercell consisting of 45 W substrate atoms), which implies that the μ_{0z} is converged at this low coverage. However, the corresponding Ba-O dimer configurations yield a μ_{0z} value that is still changing significantly even between surface coverages of 0.111 and 0.0625 MLs (4×4 surface size supercell consisting of 80 W substrate atoms). These results demonstrate that converged dipole moment values are obtained at inconveniently large supercells, having coating coverages of 0.111 ML or lower. Fortunately, the fitting procedure utilized here can approximate quite accurately the μ_{0z} parameter, which in turn can be used with $c\alpha$ to obtain the system's $\Delta\Phi$ values at any given surface-coverage value.

B. Stability and work function for $Ba_xSc_yO_z$ on W(001)

In order to understand the effects of $Ba_xSc_yO_z$ alloy surface structures on Φ for the W(001) substrate, we have attempted to determine the most stable $Ba_xSc_yO_z$ arrangement on the W surface under operating conditions. This optimization is a challenging problem as a large number of compositions and configurations are possible. However, we have taken a methodical approach (explained below) to explore the structure space and to determine the most stable surface-alloy structures. All calculations of surface formation energies are done at $T=1200$ K and pressure $P_{O_2}=10^{-8}$ Torr, as describe in Sec. II B. All work presented here is for the W(001) surface.

Initially, an arrangements of monomers (Ba, Sc, and O on the W substrate) and dimers (Ba-O or Sc-O on W) were investigated. The surface configurations tested for all monomers and dimers revealed that the surface species relaxed either over the hollow or over the corner surface sites on W(001). The hollow sites are located over the center of the W squares on the W(001) surface and directly over the body-centered atom of the W unit cell. These hollow sites form a square lattice whose side lengths equal the lattice constant of the W unit cell (see Fig. 2). The corner sites are located immediately over the surface W atoms of the W(001) surface plane (also in Fig. 2). Ba and Sc monomers were found to be most stable when bonded over the surface hollow sites for all surface coverages up to 1 ML. On the other hand, the O monomers were found to be more stable when the atomic O bonded directly over a surface W atom at the corner site, also for all surface coverages up to 1 ML. Typical formation-energy differences between the most stable (hollow or corner site) and the other high-symmetry site (corner or hollow) for approximately isolated atoms were $\sim$0.2 eV/Ba for Ba, $\sim$0.5 eV/Sc for Sc, and $\sim$0.1 eV/O for O (see Table II).

For Ba-O (and Sc-O) dimers, six main configurations were considered, motivated by the structures suggested from experiments (see Sec. II D). The six cases consist of three types of dimers, each of which can occupy either hollow or corner sites. The three types of dimers are normal (Ba on top of O normal to the W surface), flat (Ba and O second-nearest neighbors on the surface, forming a dipole nearly parallel to the W surface), and tilted (Ba and O nearest neighbors on the surface, forming a dipole at an angle to the surface—see Fig. 6). The six cases then become (i) normal dimer over corner site, (ii) normal dimer over hollow site [shown in Fig. 2(a)], (iii) flat dimer with Ba and O on corner sites, (iv), flat dimer with Ba and O on hollow sites [shown in Fig. 2(b)], (v) tilted dimer with Ba on corner and O on hollow sites, (vi) tilted dimer with Ba on hollow and O on corner sites (shown in Fig. 6). Note that dimers with Ba on the bottom and O on top were considered but they are quite unstable and enhance the W work function, opposite to what is observed experimentally. Therefore, dimers with cations on the bottom are not discussed further here.

The formation energies for all dimers studied are shown in Table II for a surface coverage of $Ba_{0.25}O_{0.25}$. For the normal dimers, the corner site was found to be the most stable, consistent with the tendency of oxygen monomers to occupy the corner sites. Normal dimers on hollow sites were originally proposed as a possible surface structure for B-type cathodes by Norman *et al.*,[24] as discussed in Sec. II D and shown in Fig. 2(a). These calculations demonstrate that even if normal dimers were to occur, they would likely occur over the corner surface sites. The flat dimers were found to be more stable with Ba and O both over corner sites, placing the O in a position consistent with its monomer energetics but forcing to Ba to occupy an unfavorable site. The flat dimers in hollow sites were originally proposed as a possible surface structure for B-type cathodes by Haas *et al.*[5] and Shih *et al.*,[25] as discussed in Sec. II D and shown in Fig. 2(b). These calculations demonstrate that even if flat dimers were to occur, they would likely occur over the corner sites. Overall the most stable dimer structure was found to be the tilted dimer

TABLE II. Monomer and dimer formation energies for $Ba_xSc_yO_z$ surface structures on W(001). W-site pairings refer to the first and the second atom of the dimer, e.g., Ba-O in the corner/hollow column is a Ba-O dimer with Ba on the corner site and O on the hollow site. All calculations are done for 0.25 ML cation coverage, e.g., $Ba_{0.25}O$ and $Ba_{0.25}O_{0.25}$.

	Corner	Hollow		
Ba	0.58	0.37		
Sc	1.75	1.23		
O	−0.60	−0.53		
	Corner/corner	Hollow/hollow	Corner/hollow	Hollow/corner
Ba-O normal	0.07	0.09	N/A	N/A
Ba-O flat	N/A	0.32	N/A	N/A
Ba-O tilted	N/A	N/A	0.05	−0.31
Sc-O normal	1.29	1.30	N/A	N/A
Sc-O flat	1.09	1.11	N/A	N/A
Sc-O tilted	N/A	N/A	0.48	0.48 (same as corner/hollow)

with O over the corner and Ba over the hollow sites of the W(001) surface. This structure allows the O and Ba to reside on the sites found to be most stable for the monomers. This tilted dimer structure is more stable than any of the other dimers by at least ~0.35 eV/dimer. Similar to the Ba-O dimers, studies with Sc dimers (also for coverage $Sc_{0.25}O_{0.25}$) predict that the tilted Sc-O dimer configuration, with Sc occupying hollow and O corner surface sites, is the stable Sc-O dimer. Corner-hollow Sc-O tilted dimers are not stable and upon relaxation, this structure evolves into the hollow-corner tilted dimer configuration (see Table II). In all cases of tilted dimers, the Ba or Sc are located farthest from the surface so that the resulting dipoles, although tilted, are still oriented in such a manner so as to point away from the W substrate and are hence capable of lowering Φ.

Based on these observations we propose that if the hot emitting surface of dispenser B-type cathodes consists of stoichiometric Ba-O dimers, then these Ba-O dimers are most likely arranged on the hot surface in a tilted fashion like the one we have identified. The implications of the stability results for the structure of the emitting surface are discussed here further and the stable tilted dimers are used for comparison of our theoretical Φ results with those obtained from experiments in Sec. III C.

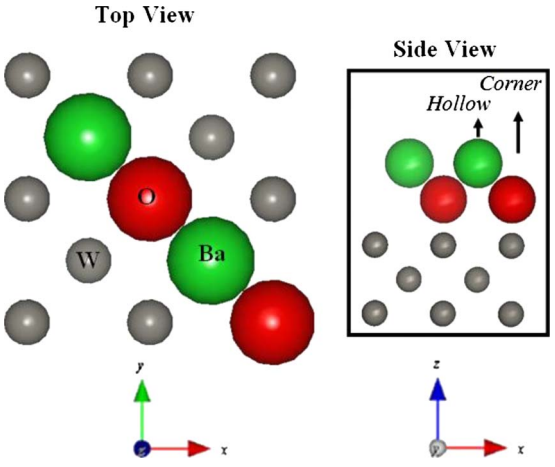

FIG. 6. (Color online) Surface structure and geometry of the most stable stoichiometric Ba-O dimer surface configuration (at stoichiometry $Ba_{0.25}O_{0.25}$) identified by *ab initio* calculations. Ba atoms are located over the hollow surface sites while O atoms are located over the corner sites (above the W atoms).

Having identified and established the stable structure of the monomer and dimer sublattices, combinations of monomers and dimers were subsequently investigated. Atomic O was introduced to the lattice at different surface coverages with each atomic O bonded over one of the W(001) surface corner atoms. The most stable arrangement was found to contain one full ML surface coverage of O, consistent with a partially oxidized surface (we say partially oxidized as the O could at most be creating W^{2+} on the nearest W atoms, which is still well below the typical valence states of 4+ and 6+ seen in stable W oxides). Structures with more than 1 ML of O were found to be less stable than structures with exactly 1 ML. Ba, Sc, and then combinations of both Ba and Sc were subsequently introduced over the stable 1 ML O surface structure, occupying the hollow sites of the surface. In total, over 70 $Ba_xSc_yO_z$ alloy surface structures, with stoichiometries ranging from $0 \leq x \leq 0.75$, $0 \leq y \leq 0.75$, and $0 \leq z \leq 2$ were investigated. Of these structures, the most stable, low Φ, and most physically relevant metastable structures (e.g., normal and tilted dimers) were identified.

The depolarization behavior of the tilted dipoles is somewhat unusual. Figure 7 compares the calculated Φ values obtained for hollow normal and tilted Ba-O and Sc-O dimers on W(001). Tilted Ba-O dimers realize their lowest Φ value (~1.8 eV) at a surface coverage of 0.25 ML. Moreover, Fig. 7 shows that for surface coverages approaching 1 ML, the tilted Ba-O dimer's Φ value does not level out in a manner analogous to that observed for normal Ba-O dimers. This is presumably due to the direct interaction of the Ba-O dimer species with their nearest surface neighbors, causing hybridization of the dimer orbitals. Figure 7 also shows that the Φ values corresponding to the tilted Sc-O dimers appear to be

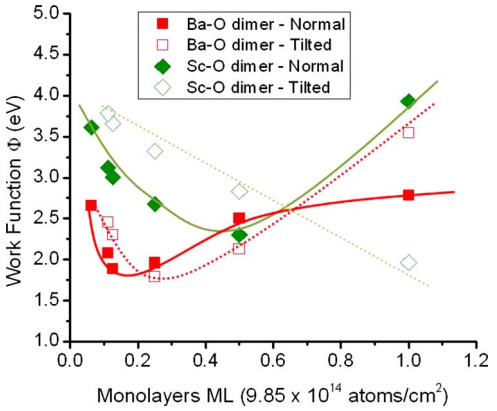

FIG. 7. (Color online) Work function, Φ, versus surface coverage (ML) for Ba-O and Sc-O surface dimer configurations obtained from *ab initio* modeling. Both normal and tilted surface dimers are included. The lines are spline interpolations and serve as a guide to the eyes.

decreasing monotonically with increasing surface coverage. A minimum Φ value of ~1.96 eV is realized for a Sc-O tilted dimer surface coverage of exactly 1 ML, indicating that for tilted Sc-O dimer configurations a minimum Φ value may be realized at denser than 1 ML Sc-O surface coverages.

The formation energies, ΔE_F, for all alloy configurations investigated were calculated using Eq. (11) in order to determine which of the $Ba_xSc_yO_z$ surface structure are thermodynamically stable under cathode operating temperature and pressure conditions. Figure 8 shows the ΔE_F for the $Ba_xSc_yO_z$ alloy surface structures investigated as a function of the total formal valence of the surface-alloy coating layer. The total formal valence is obtained by summing the typical formal valence of all the Ba, Sc, and O coating species present on the surface (the atom formal valences are taken as Ba^{2+}, Sc^{3+}, and O^{2-} so the total formal valence for $Ba_xSc_yO_z$ is given by $2x+3y-2z$). Formal valence qualitatively represents the charge balance in the surface layer and would be

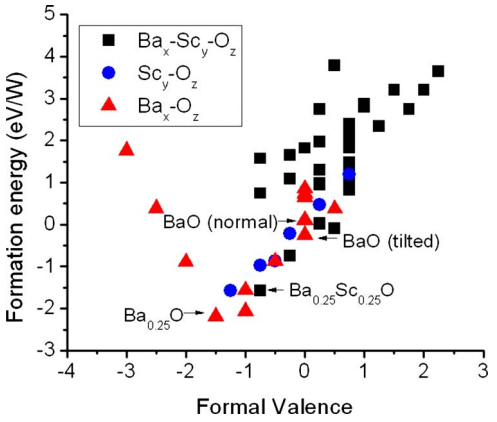

FIG. 8. (Color online) Formation energy, ΔE_F, [from Eq. (6.5)] as a function of the formal valence of various $Ba_xSc_yO_z$, Ba_xO_z, and Sc_yO_z configurations investigated computationally. Explicitly labeled in this figure are the normal and tilted Ba-O dipoles, the lowest Φ $Ba_{0.25}Sc_{0.25}O$ alloy surface structure, and the most thermodynamically stable $Ba_{0.25}O$ alloy surface structure on W(001).

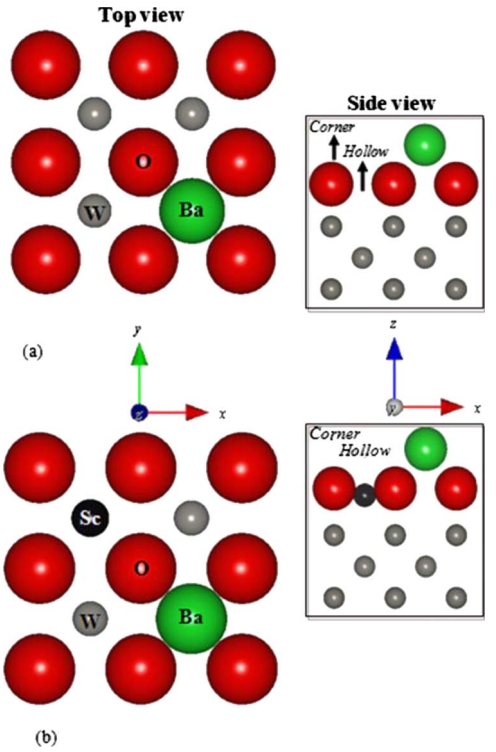

FIG. 9. (Color online) Top and side views of the 2×2 W(001) surface for (a) the $Ba_{0.25}O$ (most thermodynamically stable) and (b) the $Ba_{0.25}Sc_{0.25}O$ (lowest Φ) alloy surface configurations. Also shown are the corner and hollow surface sites. The surface O atoms are preferentially located over surface W atoms on corner sites while the Ba and Sc atoms occupy alternating hollow sites on the surface.

expected to be near zero for stable bulk compounds. The configurations shown in Fig. 8 with $\Delta E_F<0$ correspond to $Ba_xSc_yO_z$ alloy surface structures that are more stable than the BaO, Sc_2O_3, and O_2 reference states under the given operating temperature and pressure conditions ($T=1200$ K and $P_{O_2}=10^{-8}$ Torr). Moreover, it can be seen from Fig. 8 that a formal valence of ~−1.5 per W surface atom yields the lowest ΔE_F values. The reason the formal valence is negative is that the surface W atoms are donating electrons to the $Ba_xSc_yO_z$ layer. The most thermodynamically stable configuration was found to correspond to the $Ba_{0.25}O$ surface structure. The Ba occupies one of the four hollow sites of the surface situated directly over the body center W atom while the surface O atoms surrounding the Ba form a square network of corner sites (over the surface W atoms) [Fig. 9(a)]. The Φ value of the stable $Ba_{0.25}O$ configuration was determined to be 1.29 eV.[31]

Detailed investigations of Φ and stability values of the surface $Ba_xSc_yO_z$ alloy configurations have revealed the $Ba_{0.25}O$ structure as being the most thermodynamically stable compared to any of the structures (monomer, dimer, or alloy) investigated under the given operating conditions ($T=1200$ K and $P_{O_2}=10^{-8}$ Torr). The $Ba_{0.25}O$ configuration also remains the most thermodynamically stable structure of all we have calculated under room temperature ($T=300$ K) and normal air pressure ($P_{O_2}=0.2$ atm) conditions. Also la-

beled in Fig. 8 are the formation energies of the lowest Φ value coverages of the most stable normal and tilted Ba-O dipole configurations, with Φ of ~1.92 eV and ~1.8 eV, respectively. As discussed above, the tilted dipole is found to be the most stable of the stoichiometric (equal amounts of Ba and O) Ba_xO_z structures. If O is free to interact with a surface of the tilted Ba-O, it will eventually form the most thermodynamically stable $Ba_{0.25}O$ surface structure with a surface coverage of precisely 1 ML of O. Addition of any more O (more than 1 ML O surface coverage) on the surface will destabilize the structure, which can be seen in Fig. 8. Finally, Fig. 8 shows the formation energy of the scandate alloy surface structure which we identified as having the lowest overall Φ value ($Ba_{025}Sc_{0.25}O$) out of all the $Ba_xSc_yO_z$ alloy surface configurations investigated.[31] This scandate alloy surface configuration is obtained by incorporation of 0.25 ML of Sc on alternating surface hollow sites of the $Ba_{0.25}O$ surface configuration [Fig. 9(b)].

The calculated Φ values and stabilities have an important implication regarding the nature of the emitting surface of thermionic B-type dispenser cathodes. The steady-state conditions of a thermionic cathode at their operating temperatures (>800 °C) involve a balance between supply rates of reactants, formation rates of reaction product compounds, dissociation rates of compounds, and loss rates (evaporation) of atomic or molecular species. At temperatures > 800 °C, it is expected that this reaction steady state is not in thermodynamic equilibrium. Experimentally, it has been observed that the auger spectra from the hot surface of B-type cathodes can be reproduced by ~0.5 ML Ba and O on W in an approximately equal stoichiometry.[4,5] In additional support of the model that the activated cathode has a Ba_xO_z stoichiometry, our calculations with 0.125–0.25 MLs of Ba-O dimers give a work function of ~1.8–1.9 eV, very close to that observed experimentally for B-type cathodes.[4,5] On the other hand, we predict that under operating conditions the true stable phase of Ba and O on the surface of the cathode is the $Ba_{0.25}O$ compound. In fact, the formation energy of the 0.25 ML most stable tilted Ba-O dimer configuration is ~2 eV per surface W atom larger than that of the most thermodynamically stable $Ba_{0.25}O$ configuration. If stoichiometric Ba-O dimers are coating the surface of the hot cathode during operation, then it must be concluded that the emitting surface of the dispenser B-type cathode does not behave as a thermodynamic equilibrium system during operation. We propose that the Ba-O dimer structure forming on the hot surface of the cathode is due to a nonequilibrium steady-state behavior that exists during operation, dictated by the balance between Ba diffusion to, and evaporation from, the hot surface in the presence of O.

The existence of a thermodynamically stable low-Φ structure that is not on the hot emitting cathode surface during operation suggests the possibility of improving the cathode performance by stabilizing this state, or a closely related one, under operating conditions. The stabilization under operating conditions of a low-Φ structure may be a mechanism by which the presence of Sc on the surface alters the surface dynamics of the cathode system. The most stable $Ba_xSc_yO_z$ alloy for $y \neq 0$ (i.e., the $Ba_{0.25}Sc_{0.25}O$ surface structure) is essentially equivalent to the thermodynamically stable $Ba_{0.25}O$ configuration discussed earlier but with surface Sc present in the material [Fig. 9(b)]. The Φ value of this $Ba_{0.25}Sc_{0.25}O$ surface-alloy structure (1.16 eV) is the lowest we have found in the $Ba_xSc_yO_z$ alloy family. This low-Φ value agrees well with the lower range of measured Φ values for what are considered optimized scandate cathode materials, with reported Φ values typically ranging between 1.13 and 1.22 eV.[32–35] Consequently, Sc may enhance cathode performance, at least in part, by promoting the formation of a surface configuration similar to that of the most thermodynamically stable surface structure identified ($Ba_{0.25}O$) but with Sc also present in the surface of the material ($Ba_{0.25}Sc_{0.25}O$).

The stability conclusions of the previous paragraph may also provide some insights regarding the evaporation of Ba and Ba-O from the hot surface of the cathode during operation. The evaporation of Ba and Ba-O from the surface of emitting B-type thermionic cathodes is technologically important since it may limit the lifetime of the cathode and distort the low-Φ coating coverage on the surface. It has been observed that scandate cathodes, compared to conventional B-type dispenser cathodes with no Sc, exhibit less Ba and/or Ba-O evaporation while demonstrating improved lifetimes.[36] Therefore, determining whether addition of Sc may assist in lowering the Ba and Ba-O evaporation rate from the hot emitting cathode surface is of particular importance.

We have investigated the modifications of the surface binding energy (which is the energy required to remove the species from the surface) for Ba and Ba-O dimers. We considered surface configurations of Ba monomer, Ba-O normal dimer, $Ba_{0.25}O$ and $Ba_{0.25}Sc_{0.25}O$ alloy surface structures on W(001). We assume Ba may evaporate as either isolated Ba or Ba-O molecules. By comparing the energy required to remove a surface Ba atom in the Ba monomer versus the $Ba_{0.25}O$ and $Ba_{0.25}Sc_{0.25}O$ structures, we can determine whether Sc alloying can reduce the evaporation rate of Ba from the surface of an active B-type cathode. Similarly, by comparing the energy required to remove a surface Ba-O molecule in the Ba-O dimer versus the $Ba_{0.25}O$ and $Ba_{0.25}Sc_{0.25}O$ structures, we can determine whether Sc alloying is beneficial to the surface stability of an active B-type cathode by reducing the evaporation of Ba-O from the active surface. During this investigation, when atomic Ba or molecular Ba-O species are removed from the surface upon which they have stabilized and fully relaxed, the new surface structure (without the Ba or Ba-O) is allowed to fully reconstruct and relax to its most stable state.

The binding energy required to liberate a species, A, from a host material system, H, is given by

$$E_{BIN(A)} = E_{(AH)} - E_{(A)} - E_{(H)}, \tag{13}$$

where the energies for AH, A, and H are obtained directly from calculations. Table III summarizes the binding energies of one Ba atom and one Ba-O molecule for the configuration indicated. Based on these results, a number of conclusions can be inferred about the ease of Ba and Ba-O removal from the emitting surface and their implications for the surface evaporation rate of cathode materials: (a) The weakest Ba

TABLE III. Binding energies of Ba and Ba-O for the Ba, Ba-O, $Ba_{0.25}O$, and $Ba_{0.25}Sc_{0.25}O$ alloy surface configurations.

Configuration	E_{BIN}(Ba) (eV)	E_{BIN}(Ba-O) (eV)
Ba-W	−3.21	N/A
Ba-O-W (normal)	−2.45	−3.93
$Ba_{0.25}O$-W	−7.11	−7.02
$Ba_{0.25}Sc_{0.25}O$-W	−5.03	−6.57

bonding occurs for Ba-O dimers, due to the fact that Ba is only bonded to one O. (b) Surface structures with a ML of O ($Ba_{0.25}O$, $Ba_{0.25}Sc_{0.25}O$) bind both Ba and Ba-O significantly more tightly than surface structures consisting of just Ba or Ba-O dimers. This increased binding is due to the formation of the strong O-metal bonds. (c) The effect of Sc is to make Ba and Ba-O less stable in the $Ba_{0.25}Sc_{0.25}O$ configuration than in the $Ba_{0.25}O$ configuration. The addition of Sc to the most stable $Ba_{0.25}O$ surface configuration reduces the binding strength of both Ba and Ba-O on the cathode surface, likely due to both the electrostatic repulsion between the ionized Sc and Ba and the ability of Sc to provide additional stabilizing electrons to the final structure. (d) Despite the destabilization trend identified in (c), addition of Sc may actually help to stabilize Ba and Ba-O on the active surface. Note that in (c) we compare the stability of Ba and Ba-O between the $Ba_{0.25}O$ and $Ba_{0.25}Sc_{0.25}O$ configurations to assess the impact of Sc. This gives a trend of decreasing stability. However, as discussed above, the structure that appears at steady state on the active cathode is likely to be a Ba-O dimer structure and not the $Ba_{0.25}O$ structure. If we accept that Ba-O dimers are on the surface of conventional dispenser B-type cathodes, and also assume that $Ba_{0.25}Sc_{0.25}O$ is on the surface of scandate cathodes, then there is a clear increase in the binding of Ba and Ba-O. Thus it is possible that Sc doping enhances the cathode lifetime in part by stabilizing a different surface structure with greater stability against Ba/Ba-O evaporation.

Finally, it is interesting to ask whether multicomponent surface-alloy coatings can modify Φ more than their binary suballoys or if the extra species do not provide any additional gains. It was determined that the lowest Φ value (1.16 eV) for all alloy surface configurations we explored was found to correspond to the $Ba_{0.25}Sc_{0.25}O$ ternary-alloy system. By comparison, the lowest Φ value obtained with any of the binary suballoy (Ba_x-O_z or Sc_y-O_z) coatings investigated is 1.29 eV, which is larger than that obtained with the ternary-alloy system. Although the net gain for the best ternary structure is small, it demonstrates that multicomponent surface-alloy systems can modify Φ more than any of the individual suballoy components of the coating acting independently.

C. Theoretical predictions and comparison with experimental results

In this section, we compare our calculated Φ values to those for experimentally characterized $Ba_xSc_yO_z$-type surface structures, both to assess the theoretical approach utilized and to help interpret existing experimental data.

In general, it is challenging to directly compare results obtained by computational techniques (modeling idealized systems) to those obtained experimentally from real materials systems. This is particularly true when comparing Φ values because uncertainties in the experiments can make such a comparison meaningless if care and precise control of experimental conditions is not exercised. Issues making the direct comparison between theory and experiment challenging may include patchiness in the structure (and therefore Φ) on the cathode surface, inability to precisely control the amount of impurities during materials growth, uncertainty in the surface structure and composition, and sensitivity and resolution limitations of the instruments themselves that are used to characterize the materials properties of the cathodes.

The surface of an impregnated dispenser cathode is structurally and chemically very complex. Consequently, the majority of the materials characterization studies that have been reported were performed on thin-film structures grown on crystalline substrates, removing complications associated with the analysis of a polycrystalline cathode surface (see Sec. ID). The surface composition is typically controlled by allowing only known amounts of coating into the system, and then composition information is typically obtained by auger electron spectroscopy. As mentioned earlier, one of the techniques most frequently utilized for inferring surface geometry and effective coverage is LEED. However, in Ref. 35, Zagwijn *et al.* demonstrated that this approach does not accurately determine the surface coverage in a material. Using concurrently LEED and medium energy-ion spectroscopy (MEIS) for characterizing thin-film surfaces, Zagwijn *et al.* demonstrated that strong LEED $c(2\times2)$ patterns formed well before the completion of a 0.5 ML cation coverage, which is the surface coverage typically assumed when a LEED $c(2\times2)$ pattern is obtained. Specifically, for the case of Ba films on W(001), it was determined that Ba surface coverages ranging from 0.2 to 0.5 ML (as determined by MEIS) were all capable of producing strong $c(2\times2)$ LEED patterns. This observation is important as it helps explain some of the apparent discrepancies between the theoretical and experimentally obtained Φ values corresponding to seemingly identical surface systems. The details of these discrepancies are discussed below.

Figure 10 shows Φ as a function of surface coverage for Ba monomers and tilted Ba-O dimers on W(001) (the most stable dimer structures) as well as for those reported by experiments at nominally identical surface coverages. It can be seen that good overall agreement exists between theory and experiment, although there are some clear exceptions. First, we consider the Ba-O dimer systems. The Φ values for the Ba-O dimers reported by Forman[4] and Haas *et al.*[5] at a coverage of 0.5 MLs agree well with our theoretical Φ value obtained from the tilted Ba-O dipole dimer configuration for the same dimer surface coverage. Haas *et al.* infer the surface coverage by performing LEED on a Ba-O thin film on W(001) while Forman from measurements on a polycrystalline W substrate coated with a thin Ba-O film. The good agreement between theory and experiment also holds when comparing Zagwijn *et al.*'s[35] low-Φ oxidized 0.27 ML Ba

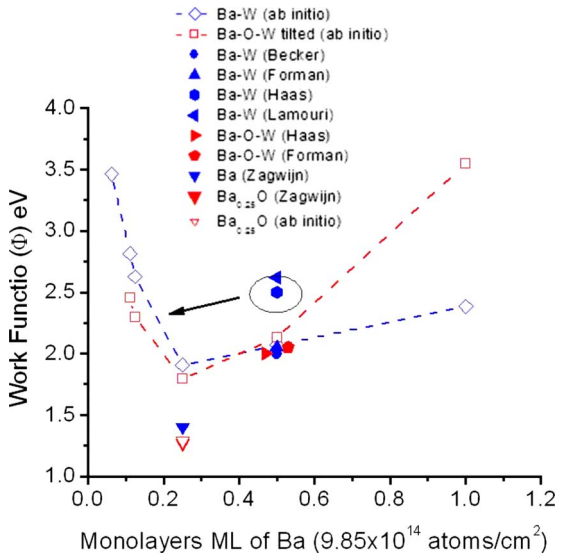

FIG. 10. (Color online) Work function, Φ, as a function surface coverage for Ba monomer and Ba-O (tilted) dimer surface structures on W(001) obtained by *ab initio* calculations and from experiments. See text for citations. Note that the experimental values with Φ ~ 2 eV and 0.5 ML Ba coverage have been shifted slightly along the abscissa to make viewing easier.

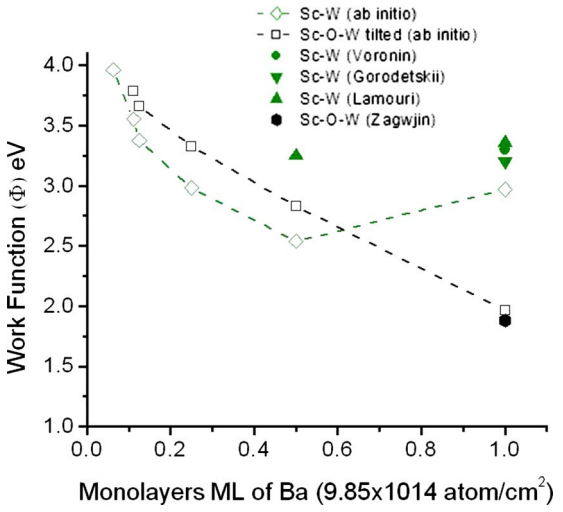

FIG. 11. (Color online) Work function, Φ, as a function surface coverage for Sc monomer and Sc-O (tilted) dimer surface structures on W(001) obtained by *ab initio* calculations and from experiments.

surface structure with that of our $Ba_{0.25}O$ configuration. Zagwijn *et al.*'s structure was obtained when the W(001) substrate, initially precovered by 0.27 ML of Ba, was exposed to O gas. The total amount of O adsorbed on the surface during exposure was not determined but it is plausible that the two structures, by virtue of their almost identical Ba surface coverage, Φ values, and similar monolayer-type surface coating, are indeed the same.

Switching our discussion to the Ba on W(001) system, we can see that our 0.5 ML theoretical Φ values agree well with those reported by Forman[4] and Becker.[37] On the other hand, disagreement exists between our Φ values and those reported by Haas *et al.*[5] and Lamouri *et al.*[38] for the same 0.5 ML Ba surface coverage. We believe the reason for the discrepancy between Haas *et al.*'s 0.5 ML Ba Φ value and ours can be explained as follows. Haas *et al.* deposited Ba on the W(001) substrate until the 1×1 LEED structure of the underlying W substrate disappeared, after which they annealed the sample so that a $c(2\times2)$ LEED pattern was observed from the surface. As mentioned above, Zagwijn *et al.* demonstrated that a strong $c(2\times2)$ LEED pattern may not necessarily correspond to a Ba surface coverage of 0.5 ML, and can be produced by a surface coverage as low as 0.2 ML. A shift to a Ba surface coverage of 0.2 MLs in Fig. 10 would result in the good agreement between Haas *et al.*'s Φ value (his error bar is ~0.4 eV) and ours. The discrepancy with Lamouri *et al.*[38] could be explained by noticing in Fig. 10 that the difference in our Ba-W Φ values between the 0.5 and 1 ML Ba coverages is almost identical to Lamouri *et al.*'s for the same nominal surface coverages. Moreover, the converged Ba Φ value for high Ba coverages in Lamouri *et al.* appears to be ~0.5 eV larger than the value typically reported.[14] These facts seem to suggest that Lamouri *et al.*'s Φ values may simply be shifted up by ~0.5 eV, perhaps due to a measurement calibration issue. If we allow for such a shift, then our values and Lamouri *et al.*'s are in good agreement. The final discrepancy is the very low-Φ value obtained for ~0.25 MLs of Ba on W(001) reported by Zagwijn *et al.* While we cannot match this value for any pure Ba coverage, it is possible that this discrepancy is due to trace amounts of O on the surface, yielding a configuration similar to the very low-Φ $Ba_{0.25}O$ alloy surface structure. As a last remark, it is interesting to note that a comparable reduction in Φ can be obtained by 0.25–0.5 MLs of Ba as well as tilted Ba-O dimers on W(001), in agreement with previous reports[22] indicating that the reduction in Φ realized by 0.5 MLs of Ba as well as Ba-O were almost identical.

Figure 11 shows Φ as a function of surface coverage for Sc monomer and tilted Sc-O dimer surface configurations on W(001) (most stable structures) and those reported by experiments for apparently identical nominal surface-coverage structures. Again good overall agreement exists between theory and experiments, except for some exceptions that can be explained. More specifically, the Φ value of our 1 ML $Sc_{0.5}O_{0.5}$ surface structure is in good agreement with that reported by Zagwijn *et al.*[35] for a 1ML Sc coverage. The low-Φ value was attributed by Zagwijn *et al.* to be due to contamination of the Sc film by residual O, which is consistent with the fact that our Sc-O results match results from Zagwijn *et al.*'s but not our pure Sc layer results. A relatively good agreement exists between our 1 ML Sc on W(001) structure Φ value with those reported by Voronin[39] and Gorodetskii *et al.*[40] (their error is ~0.2 eV) and Lamouri *et al.*[41] for the same nominal Sc surface coverage on W(001). The Φ difference between theory and experiment at 1 ML Sc is ~0.2 eV. On the other hand, Lamouri *et al.*'s[41] Φ value reported for a 0.5 ML Sc surface coverage on W(001) deviates by over 0.7 eV from our Φ value for a structure with presumably the same nominal surface coverage. An incorrectly inferred Sc surface coverage due to reliance on the $c(2\times2)$ LEED pattern is a possible reason for the observed discrepancy.

Finally, a scandium-containing ternary-alloy surface structure on W(001), with a Φ value of 1.18 eV was also reported by Zagwijn *et al.*[35] but the nominal stoichiometry of this thin-film scandate structure was determined to be $Ba_1Sc_1O_{1.5}$. Detailed analytical studies and characterizations were not performed on this structure by the authors but it is possible that our $Ba_{0.25}Sc_{0.25}O$ structure may have been present in that material, contributing to the almost identically low-Φ value reported for these two structures.

IV. SUMMARY AND CONCLUSIONS

In summary, *ab initio* modeling techniques and thermodynamic theory were utilized to investigate the structure, the Φ, and the stability of $Ba_xSc_yO_z$ on W(001) surface-alloy structures.

It has been demonstrated that surface depolarization effects can be calculated using DFT-based computational techniques. For many cases, simple fitting to an analytic depolarization expression can be used to obtain the complete depolarization curve (dipole moment versus coverage) from relatively few DFT calculations. The fitted model can be used to predict Φ versus coverage for arbitrary coverage values, determine the net dipole moment per isolated surface species, μ_{0z}, and estimate the surface species dipole moment effective polarizability, α.

The formation energy was used as a guide for determining plausible surface-alloy configurations on the W(001) surface. It was found that the normally oriented Ba-O on W(001) dipole dimer layer, believed to be responsible for the lowered Φ observed in B-type thermionic dispenser cathodes, is not thermodynamically stable under typical cathode operating conditions. Among Ba_xO_z stoichiometry configurations, a tilted Ba-O dimer surface configuration was found to be the most stable. The most thermodynamically stable phase of the coating on the W surface was identified by calculations to be the $Ba_{0.25}O$ surface configuration, which possesses a significantly lower Φ value than any of the Ba-O dimer configurations. This stability of the $Ba_{0.25}O$ structure, combined with the fact that it does not seem to be consistent with measured Φ values or surface structures on active B-type cathodes, suggests that a nonequilibrium steady state dominates the surface of active B-type cathodes. Addition of Sc yields new stable compounds with even lower Φ values. The most stable Sc-containing surface structure that we calculated was $Ba_{0.25}Sc_{0.25}O$. This structure is quite similar to the $Ba_{0.25}O$ structure, and it is hypothesized that addition of Sc to the active B-type surface cathode structure stabilizes the $Ba_{0.25}Sc_{0.25}O$ structure on the surface under operating conditions, leading to improved performance and stability of Sc-doped cathodes. The $Ba_{0.25}Sc_{0.25}O$ alloy structure is seen to possess a lower Φ value (1.16 eV) than any of its binary suballoys, demonstrating that multicomponent alloying can produce surface structures with Φ lower than that of its individual components.

Finally, a detailed comparison is made between the Φ values from the $Ba_xSc_yO_z$ on W(001) alloy surface structures obtained by *ab initio* calculations and those obtained experimentally from similar structures. Good overall agreement exists between the theory and experiments. A few discrepancies exist between the theory and experiments but guided by the theoretical results a number of possible explanations were proposed to account for the discrepancies. The studies presented here demonstrate how *ab initio* methods, through calculation of structure, work function, and stability, are a powerful tool for understanding fundamental physics, interpreting experiments, and aiding in development related to electron emission cathodes.

ACKNOWLEDGMENT

This work is supported by a US DoD MURI04 AFOSR grant on the Nano-physics of High Current Density Cathodes and Window Breakdown.

*Present address: L-3 Communications-Electron Devices Division, 960 Industrial Rd., San Carlos, CA 94070, USA.

[1] *Modern Microwave and Millimeter-Wave Power Electronics*, edited by R. J. Barker, J. H. Booske, N. C. Luhmann, and G. S. Nusinovich (IEEE Press, Wiley-Interscience, Piscataway, NJ, 2005).
[2] *Vacuum Microelectronics*, edited by W. Zhu (Wiley-Interscience, Hoboken, NJ, 2001).
[3] J. Hölzl and F. K. Schülte, *Work Function of Metals* (Springer-Verlag, Berlin, 1979).
[4] R. Forman, Appl. Surf. Sci. **2**, 258 (1979).
[5] G. A. Haas, A. Shih, and C. R. K. Marrian, Appl. Surf. Sci. **16**, 139 (1983).
[6] V. Vlahos, D. Morgan, and J. H. Booske, Appl. Phys. Lett. **91**, 144102 (2007).
[7] D. Shiffler, J. Heggemeier, M. LaCour, K. Golby, and M. Ruebush, Phys. Plasmas **11**, 1680 (2004).
[8] G. Kresse and J. Furthmüller, Comput. Mater. Sci. **6**, 15 (1996).
[9] P. Hohenberg and W. Kohn, Phys. Rev. **136**, B864 (1964).
[10] J. P. Perdew, K. Burke, and Y. Wang, Phys. Rev. B **54**, 16533 (1996).
[11] G. Kresse and D. Joubert, Phys. Rev. B **59**, 1758 (1999).
[12] H. J. Monkhorst and J. D. Pack, Phys. Rev. B **13**, 5188 (1976).
[13] VASP manual, http://cms.mpi.univie.ac.at/vasp/vasp/vasp.html
[14] *CRC Handbook of Chemistry and Physics*, 89th ed. (CRC, Cleveland, 2008-2009).
[15] J. Taylor and I. Langmuir, Phys. Rev. **44**, 423 (1933).
[16] L. Gaines, *Insoluble Monolayers at Liquid-Gas Interfaces* (Wiley-Interscience, New York, 1966).
[17] J. Topping, Proc. Roy. Soc. London, Ser. A **114**, 67 (1927).
[18] E. Heifets, J. Ho, and B. Merinov, Phys. Rev. B **75**, 155431 (2007).
[19] L. Wang, T. Maxisch, and G. Ceder, Phys. Rev. B **73**, 195107 (2006).
[20] Y.-L. Lee, J. Kleis, J. Rossmeisl, and D. Morgan, Phys. Rev. B **80**, 224101 (2009).

[21] Y. Wang, J. Wang, W. Liu, K. Zhang, and J. Li, IEEE Trans. Electron Devices **54**, 1061 (2007).
[22] R. Forman, J. Appl. Phys. **47**, 5272 (1976).
[23] G. E. Moore and H. W. Allison, J. Chem. Phys. **23**, 1609 (1955).
[24] D. Norman, R. A. Tuck, H. B. Skinner, P. J. Wadsworth, T. M. Gardiner, I. W. Owen, C. H. Richardson, and G. Thornton, Phys. Rev. Lett. **58**, 519 (1987).
[25] A. Shih, C. Hor, W. Elam, J. Kirkland, and D. Mueller, Phys. Rev. B **44**, 5818 (1991).
[26] L. A. Hemstreet, S. R. Chubb, and W. E. Pickett, J. Vac. Sci. Technol. A **6**, 1063 (1988).
[27] L. A. Hemstreet, S. R. Chubb, and W. E. Pickett, Phys. Rev. B **40**, 3592 (1989).
[28] W. Müller, Tech. Dig.-Int. Electron Devices Meet. **1991**, 399.
[29] L. A. Hemstreet and S. R. Chubb, Phys. Rev. B **47**, 10748 (1993).
[30] *Electronics and Electron Physics*, edited by P. Zalm and L. Marton (Academic, New York, 1968), Vol. 25.
[31] V. Vlahos, Y. L. Lee, J. H. Booske, D. Morgan, L. Turek, M. Kirshner, R. Kowalczyk, and C. Wilsen, Appl. Phys. Lett. **94**, 184102 (2009).
[32] S. Taguchi, T. Aida, and S. Yamamoto, IEEE Trans. Electron Devices **31**, 900 (1984).
[33] S. Yamamoto, T. Yaguchi, S. Sasaki, and I. Watanabe, Jpn. J. Appl. Phys. **28**, L865 (1989).
[34] G. Gärtner, P. Geittner, H. Lydtin, and A. Ritz, Appl. Surf. Sci. **111**, 11 (1997).
[35] P. M. Zagwijn, J. W. M. Frenken, U. van Slooten, and P. A. Duine, Appl. Surf. Sci. **111**, 35 (1997).
[36] G. Gärtner and D. Barratt, Appl. Surf. Sci. **251**, 73 (2005).
[37] J. A. Becker, Trans. Am. Electrochem. Soc. **55**, 153 (1929).
[38] A. Lamouri and I. L. Krainsky, Surf. Sci. **278**, 286 (1992).
[39] V. B. Voronin, Fiz. Tverd. Tela (Leningrad) **9**, 2242 (1967) [Sov. Phys. Solid State **9**, 1758 (1968)].
[40] D. A. Gorodetskii and A. A. Yas'ko, Fiz. Tverd. Tela (Leningrad) **11**, 2513 (1969) [Sov. Phys. Solid State **11**, 2028 (1970)].
[41] A. Lamouri, I. L. Krainsky, A. G. Petukhov, W. R. L. Lambrecht, and B. Segall, Phys. Rev. B **51**, 1803 (1995).